agriculture

MDPI

Article

Optimization of Stevia Residue Fermentation Process via Response Surface Methodology and Evaluation of Its Effects on Laying Hens

Fumeng He [1,†], Binghua Qin [2,†], Yongqi Wang [1], Md. Abul Kalam Azad [2], Yanzhong Feng [3], Xiangfeng Kong [1,2,*] and Fenglan Li [1,*]

[1] College of Life Sciences, Northeast Agricultural University, Harbin 150030, China; hefumeng@neau.edu.cn (F.H.); wangyongqi199910@outlook.com (Y.W.)
[2] Hunan Provincial Key Laboratory of Animal Nutritional Physiology and Metabolic Process, National Engineering Laboratory for Pollution Control and Waste Utilization in Livestock and Poultry Production, Institute of Subtropical Agriculture, Chinese Academy of Sciences, Changsha 410125, China; qinbinghua23@mails.ucas.ac.cn (B.Q.); azadmak@isa.ac.cn (M.A.K.A.)
[3] Institute of Animal Husbandry, Heilongjiang Academy of Agricultural Sciences, Harbin 150086, China; lixiang@haas.cn
* Correspondence: nnkxf@isa.ac.cn (X.K.); lifenglan@neau.edu.cn (F.L.)
† These authors contributed equally to this work.

Abstract

Stevia residue (SR), a typical by-product of the stevia industry, is rich in organic matter and has great potential as a feed resource. However, its high fiber content and low utilization efficiency limit its practical application in poultry production. To improve the nutritional value and application potential of SR, this study first optimized the fermentation conditions of SR using response surface methodology (RSM) with chlorogenic acid as the key optimization index and then investigated the effects of different doses of SR and fermented SR (FSR) on laying performance, egg quality, antioxidant capacity, and immunity in laying hens. Six fermentation parameters, including pH, solid-to-liquid ratio, temperature, inoculation quantity, brown sugar addition, and soybean meal addition, were first screened using single-factor experiments and then optimized with RSM. Subsequently, 560 laying hens were randomly divided into seven groups and fed a basal diet supplemented with 0, 0.5%, 1.0%, and 1.5% of either SR or FSR for 28 days. The results showed that the optimal fermentation conditions were a solid-to-liquid ratio of 75.6%, brown sugar addition of 2.7%, temperature of 25 °C, inoculation quantity of 3%, and fermentation time of 9 days. In the animal study, dietary 0.5% SR and FSR reduced average daily feed intake and eggshell strength, whereas the plasma total antioxidant capacity was enhanced in all (SR or FSR) supplemented groups ($p < 0.05$). Moreover, plasma immunoglobulin (Ig) A level was increased in the 1.0–1.5% SR and 1.5% FSR groups, and plasma IgY was elevated in the 1.0% SR group ($p < 0.05$). Our results suggested that SR fermentation was effectively optimized through RSM, and dietary FSR supplementation at 1.0% improved the health of laying hens, representing the optimal inclusion level.

Keywords: feed additive; fermentation; laying hens; response surface methodology; stevia residue

Check for updates

Academic Editor: Petru Alexandru Vlaicu

Received: 14 April 2026
Revised: 30 April 2026
Accepted: 30 April 2026
Published: 4 May 2026

Copyright: © 2026 by the authors. Licensee MDPI, Basel, Switzerland. This article is an open access article distributed under the terms and conditions of the Creative Commons Attribution (CC BY) license.

1. Introduction

Plant-derived feed additives have gained increasing attention in animal production. Rich in bioactive compounds like polyphenols, alkaloids, and flavonoids, these additives

confer notable health-promoting characteristics [1], including growth promotion [2] and immune regulation, as well as maintaining the gut microbiota in animals [3,4]. With the rising demand for safe, efficient feed additives amid limited resources, developing novel plant-based additives is of great significance for utilizing non-conventional resources and supporting the green and sustainable development of the livestock industry.

Stevia (*Stevia rebaudiana*) is a perennial herbaceous plant from the *Asteraceae* family, rich in bioactive compounds such as glycosides [5], chlorogenic acids [6], and flavonoids, and it exhibits physiological functions, including antibacterial, anti-inflammatory, immune performance-enhancing, and gut microbiota-regulating activities [7]. Stevia residue (SR), a by-product generated after the extraction of stevioside from stevia, retains high nutritional value [8]. Research evidence has indicated that diet supplemented with stevia and its by-product can enhance poultry health by enhancing production performance, and thereby optimize product quality. For example, Tang et al. [9] reported that diets supplemented with SR improved production performance and egg quality in laying hens, while enhancing immune function, antioxidant capacity, and intestinal health. Similarly, a commercial-based diet supplemented with 80 ppm stevia-based sweetener improved body weight gain and immune response in broilers at the market age [10]. Moreover, yellow-feathered broilers supplemented with stevia extract exhibited enhanced growth performance, antioxidant and immune capacity, and intestinal health, with an optimal concentration range of 100 to 200 mg/kg [8]. However, the current disposal methods for SR, such as incineration and composting, result in significant economic losses and environmental pollution [11]. Therefore, an appropriate approach is urgently needed to develop efficient methods for SR resource utilization to alleviate its environmental pollution and economic losses, and further explore its potential as a functional feed additive to promote the healthy breeding of poultry.

Fermentation is one of the effective approaches for the valorization of agricultural by-products [11]. This process not only reduces crude fiber content but also enriches bioactive compounds, thereby improving the nutritional value of agricultural by-products [12,13]. Optimizing fermentation conditions is key to enhancing substrate utilization efficiency and final product quality factors, which directly influence the process value [14]. The single-factor method, which fixes other variables while varying one at a time, allows for rapid screening of the suitable ranges for key conditions such as temperature and pH. Although convenient to operate and useful for laying the foundation for subsequent optimization, this method fails to reflect the interactions between factors [15]. Response surface methodology (RSM), based on regression models, investigates the comprehensive effects of multiple variables and their interactions on results through a limited set of experiments, enabling accurate localization of the wide range of optimal parameter combinations, and thereby overcoming the limitations of the single-factor method [16]. Therefore, a two-step strategy of "single-factor screening followed by RSM optimization" is an ideal and efficient approach, balancing preliminary efficiency with final precision.

In this study, single-factor experiments and RSM were used to optimize the fermentation parameters of SR, with chlorogenic acid (CA) content selected as the key response variable for optimization. CA was selected because it is the most abundant functional polyphenol in SR and serves as a representative marker for polyphenolic bioactivity [17]. Furthermore, research evidence indicated that CA exhibits antioxidant, anti-inflammatory, and immunomodulatory effects, which are directly relevant to the health and performance of laying hens [17]. Subsequently, the nutritional composition, microbial community, and metabolite profiles of the fermented stevia residue (FSR) were analyzed to elucidate the changes induced by the optimized fermentation process. Furthermore, SR and FSR were incorporated into the diets of laying hens to evaluate their effects on laying performance,

immune function, and antioxidant status. The FSR was expected to outperform SR in layer production, as microbial fermentation can release greater amounts of polyphenolic substances such as CA and enrich beneficial microbial metabolites. Unlike previous studies, which mainly focused on the simple feeding application of SR, the present study systematically optimized the fermentation parameters of SR and further evaluated the comparative effects of SR and FSR at different doses in laying hens to explore dose-dependent responses. In particular, the work linked changes in microbial community and metabolite profiles to the antioxidant capacity and immune function of laying hens, offering a novel perspective for achieving an in-depth understanding of SR application. Thus, this research aimed to optimize the solid-state fermentation conditions of SR, characterize the functional changes in FSR, and evaluate their effects on the physiological health of laying hens. The findings integrate fermentation optimization, compositional changes, and *in vivo* effects to provide a systematic understanding of the application value of FSR, supporting its use as a plant-based feed additive in layer production.

2. Materials and Methods

2.1. Preparation of Stevia Residue and Microbial Agents

The SR was obtained from the Institute of Subtropical Agriculture, Chinese Academy of Sciences (Changsha, China). The microbial agent, comprising *EM bacteria*, *Phanerochaete chrysosporium* AFRC34, and *Phanerochaete chrysosporium Burdsall* AFRC45 in a ratio of 1:1:1, was provided by the Heilongjiang Province High-Quality Agricultural Functional Microbial Engineering Technology Research Center (Harbin, China).

2.2. Optimization of Cell Wall-Breaking Fermentation Process for Stevia Residue

For single-factor experiments, six parameters, including inoculation quantity, temperature, solid-to-liquid ratio, brown sugar addition, soybean meal addition, and initial pH, were determined to assess their effects on CA content in FSR. In this study, the solid-to-liquid ratio was defined in volume-to-weight (v/w) terms, with 75 mL of distilled water added to 100 g of dry SR to achieve a standardized ratio of 75% (v/w) for fermentation. The basic extraction conditions were as follows: 1 g of freeze-dried SR sample was subjected to ultrasonic extraction using an ultrasonic cleaner (Scientz-1000C, Xinzhi Biotechnology Inc., Ningbo, China) under constant conditions of 60% ethanol, a solid-to-liquid ratio of 1:50 (w/v), a temperature of 60 °C, and ultrasonic power of 500 W. The resulting extract was then filtered, diluted, and analyzed. The CA content was determined using commercial assay kits (Harbin Tai Sige Biotechnology Co., Ltd., Harbin, China) on a microplate reader (Multiskan Sky with Touch Screen, Thermo Scientific Spectrophotometer, Life Technologies Holdings Pte. Ltd., Singapore). In each experiment, only one variable was changed at a time, while all others were kept constant. The optimal condition identified in the earlier single-factor experiment was applied as baseline values for the subsequent experiments. The detailed experimental scheme of the single-factor is presented in Table S1.

Based on the results of single-factor experiments, three parameters, including solid-to-liquid ratio (A), brown sugar addition (B), and temperature (C), were selected to conduct response surface optimization. Using Design-Expert 13 software, a Box–Behnken design (BBD) was applied, consisting of seventeen experimental runs, including twelve factorial points and five center points. The detailed experimental conditions for the response surface optimization are presented in Table S2.

2.3. Morphological Observation and Nutrient Composition Analysis of Fermented Stevia Residue

After identifying the optimal fermentation conditions, SR was subjected to solid-state fermentation for 15 days. Distilled water and microbial agent were added at a proportion

of 3% (v/w) based on the dry weight of SR to ensure proper moisture and microbial colonization conditions. Samples were collected at 0, 3, 6, 9, 12, and 15 days of fermentation and stored at −80 °C for further analysis.

The morphological structure of all samples was observed using a scanning electron microscope (FESEM; model SU8010; Hitachi, Japan). The activities of laccase and cellulase in FSR were determined on a microplate reader (Multiskan Sky with Touch Screen, Thermo Scientific Spectrophotometer, Life Technologies Holdings Pte., Ltd., Singapore) using commercial assay kits (Harbin Tai Sige Biotechnology Co., Ltd., Harbin, China).

The content of crude fat, crude fiber, and crude ash was analyzed according to the guidelines outlined by the National Standard of the People's Republic of China GB/T 6433-2006 [18], GB/T 6434-2006 [19], and GB/T 6438-2007 [20], respectively. The content of soluble sugars was determined using the sulfuric acid–anthrone method. The acidic and alkaline soluble proteins were extracted using the methods previously described by Wang et al. [21] and Zhai et al. [22], respectively. Then, the content of acidic and alkaline soluble proteins was determined via Coomassie Brilliant Blue staining.

2.4. 16S and 18S rRNA Gene Sequencing of Fermented Stevia Residue

For 16S rRNA gene sequencing, the bacterial DNA from FSR was extracted using a TIANamp Soil DNA Kit according to the manufacturer's instructions. The V3−V4 hypervariable regions of the bacterial 16S rRNA gene were then amplified using the universal primers 341F (5′-ACTCCTACGGGAGGCAGCAG-3′) and 806R (5′-GGACTACHVGGGTWTCTAAT-3′). Amplicon sequencing and bioinformatics analysis were performed by Boyue Zhihe Biotechnology Co., Ltd. (Wuhan, China), on an Illumina HiSeq PE250 platform (Illumina; San Diego, CA, USA).

The resulting sequencing data were processed using the Quantitative Insights into Microbial Ecology 2 (QIIME2) pipeline. Afterward, Divisive Amplicon Denoising Algorithm 2 (DADA2) was used to determine amplicon sequence variants (ASVs) through sequence denoising. The taxonomy and annotation of ASVs were based on the SILVA database. The diversity plugin was used to determine the alpha-diversity indices, including Chao1, Observed_species, Shannon index, Simpson index, Pielou-evenness, Faith_pd, and Good's coverage. A principal coordinate analysis (PCoA) map based on the Bray–Curtis distance was used to determine beta-diversity. Taxonomic differences at the phylum and genus levels were determined using the Kruskal–Wallis test. Finally, linear discriminant analysis (LDA) effect size (LEfSe) analysis was performed to identify statistically significant biomarkers among the different groups.

For 18S rRNA gene sequencing, the microbiota DNA was subjected to PCR amplification using the primers F (5′-CCAGCASCYGCGGTAATTCC-3′) and R (5′-ACTTTCGTTCTTGATYRA-3′), which target the V4 regions of the fungal 18S rRNA. The subsequent library construction, sequencing platform, and paired-end sequencing conditions were identical to those used for 16S rRNA gene sequencing.

2.5. Metabolite Analysis of Fermented Stevia Residue

The FSR samples were ground into powder and homogenized with 400 µL of a pre-cooled methanol/acetonitrile/water solution (4:4:2, $v/v/v$). The mixture was stored at −20 °C for 60 min, and then centrifuged at 14,000× g for 20 min at 4 °C. The supernatant was collected and vacuum-dried. The dried residue was reconstituted in 100 µL of an acetonitrile aqueous solution (acetonitrile/water = 1:1, v/v) and then re-dissolved. After vortexing and centrifuging (14,000× g for 15 min at 4 °C), 2 µL of the final supernatant was transferred to a vial for LC-MS analysis.

Metabolite separation was performed on an ACQUITY UPLC BEH C18 column (1.7 µm, 100 × 2.1 mm; Waters; Milford, MA, USA). The column temperature was maintained at 40 °C with a flow rate of 0.3 mL/min. The injector volume was 5 µL. The mobile phases contained 0.1% formic acid–water solution (A) and acetonitrile (B). The following linear gradients were used: 0–0.5 min with 5% B, 0.5–1.0 min with 5% B, 1.0–9.0 min with 5–100% B, 9.0–12.0 min with 100% B, and 12.0–15.0 min with 5% B.

The MS parameters for ion/metabolite detection were as follows: Ion Source Gas1 (Gas1), 60; Ion Source Gas2 (Gas2), 60; curtain gas (CUR), 30; source temperature, 320 °C; and IonSpray Voltage Floating (ISVF), +3500 or −3500 V in positive and negative ion modes, respectively. The MS scan range (m/z) was set to 80–1200 Da with a resolution of 17,500. Accumulation time was 0.20 s/spectrum for MS scans and 0.05 s/spectrum for product ion scans. Metabolite analysis was conducted using Information Dependent Acquisition (IDA) mode. The collision energy was set at 35 ± 15 eV. The parameters of IDA were: exclude isotopes within 4 Da, and 6 candidate ions to monitor per cycle.

The raw data collected by mass spectrometry were subjected to data preprocessing, including peak extraction, alignment, correction, and standardization using Compound Discoverer 3.0 (Thermo Fisher Scientific, Waltham, MA, USA) software. Metabolite structure identification was carried out using databases including BioCyc, HMDB, Metlin, HFMDB, and Lipidmaps.

2.6. Animals and Feeding Management

The experiment was conducted and data were collected in 2022–2023. A total of 560 healthy laying hens (50-week-old) were randomly divided into seven groups. Each group consisted of eight replicates with 10 hens in each replicate. The birds in the control group were fed a basal diet, while birds in the treatment groups were fed a basal diet supplemented with 0.5%, 1.0%, and 1.5% of either SR or FSR. The trial lasted 28 days. Each replicate was housed in two adjacent wire cages with five birds per cage, and feed and water were made freely available to the birds throughout the study. The rearing environment consisted of a well-ventilated room with controlled temperature (18–23 °C) and humidity (55–65%), and a diurnal cycle of 16 h light and 8 h darkness. The composition and nutrient levels of the basal diet are presented in Table S3.

2.7. Production Performance and Egg Quality Determination

The number and weight of eggs were recorded daily to calculate the average laying rate (ALR) and average egg weight (AEW). Feed intake and leftovers were recorded weekly for each replicate to calculate the average daily feed intake (ADFI) and feed-to-egg ratio (FER).

On day 28 of the trial, three eggs from each replicate were collected for egg quality analysis. Albumen height, egg yolk color, and Haugh units were measured using a multifunction egg quality analyzer (Orka Food Technology Ltd., Ramat Hasharon, Israel). Eggshell strength was measured with an Egg Force Reader 01 (Orka Food Technology Ltd., Ramat Hasharon, Israel). Eggshell thickness was evaluated by taking the mean of three measurements obtained at standardized positions: blunt end, equatorial region, and the sharp end. An electronic digital Vernier caliper (Shanghai Shenhan Measures Co., Ltd., Shanghai, China) was used to measure the maximum horizontal and vertical diameters to calculate the egg shape index.

2.8. Plasma Antioxidant Capacity and Immune Function Analysis

Blood samples (5 mL) were collected from the wing veins of hens (n = 5) into heparinized tubes and then centrifuged at 4000× g for 10 min to obtain plasma. The plasma antioxidant capacity parameters (including total antioxidant capacity, T-AOC; glutathione peroxidase, GSH-PX; and malondialdehyde, MDA) and plasma immune parameters (in-

cluding immunoglobulin (Ig) A, IgM, and IgY, and chicken infectious coryza antibody (IC Ab)), were determined using commercial assay kits (Harbin Tai Sige Biotechnology Co., Ltd., Harbin, China) following the manufacturer's instructions on a Microplate Reader (Multiskan Sky with Touch Screen, Thermo Scientific Spectrophotometer, Life Technologies Holdings Pte. Ltd., Singapore).

2.9. Statistical Analysis

The data were sorted using Microsoft Excel 2016 and subsequently analyzed with SPSS 26.0 software (IBM Inc., Chicago, IL, USA). Data normality was assessed using the Shapiro–Wilk test, and homogeneity of variances was verified using Levene's test as part of the one-way ANOVA procedure. For datasets that met both assumptions of normality and homogeneity of variances, significant differences were analyzed using one-way ANOVA followed by Tukey's post hoc test. Additionally, pairwise comparisons between SR and FSR at the same supplemental dose were performed using an independent samples *t*-test. For other datasets, the Kruskal–Wallis test was used for nonparametric analysis. To analyze the effects of SR and FSR in laying hen diets, the supplemental dose was treated as a continuous variable for each additive type, and four gradient levels were used to conduct linear and best-fit quadratic regression models. The RSM was performed using Design-Expert 13 software, and figures were generated using Origin 2021. Data are presented as means with their standard error of the mean (SEM), and differences are considered statistically significant at $p < 0.05$.

3. Results

3.1. Pre-Optimization of Fermented Stevia Residue Using Single-Factor Experiments

As shown in Figure 1, all six parameters (brown sugar addition, inoculation quantity, pH, soybean meal addition, solid-to-liquid ratio, and temperature) affected the CA content in FSR ($p < 0.05$) compared with the SR. As shown in Figure 1A, the effect of brown sugar addition on CA content exhibited a trend of initial decrease, followed by an increase, and eventual decrease. As the brown sugar addition increased to 4%, the CA content in FSR reached its peak (4.73 mg/g). However, upon further increasing the brown sugar addition, the decrease in CA content was not significant ($p > 0.05$).

As shown in Figure 1B, the effect of inoculant quantity on the CA content showed an initial increase, followed by a plateau. When the inoculant quantity changed from 1% to 3%, the CA content in FSR increased from 3.58 to 4.47 mg/g ($p < 0.05$). However, further increasing the inoculation quantity did not result in a significant increase in the CA content ($p > 0.05$).

As shown in Figure 1C, D, both the initial pH value and the soybean meal addition showed an increasing trend for CA content. No significant variation ($p > 0.05$) in CA content was observed in the FSR across different initial pH values or soybean meal addition. Accordingly, the initial pH value and the soybean meal addition were not considered for subsequent experiments. The absence of significant variation in these two factors likely stems from the narrow gradient ranges employed in the single-factor experiments. Thus, future studies are recommended to expand these testing ranges to better assess their potential impact on fermentation efficiency, thereby facilitating a more comprehensive understanding and optimization of the fermentation process.

As shown in Figure 1E, the effect of solid-to-liquid ratio on the CA content exhibited an initial increase followed by a decrease. The highest CA content (4.56 mg/g) was achieved at an 80% solid-to-liquid ratio, and there were significant changes observed compared with the 60 and 100% ratio ($p < 0.05$).

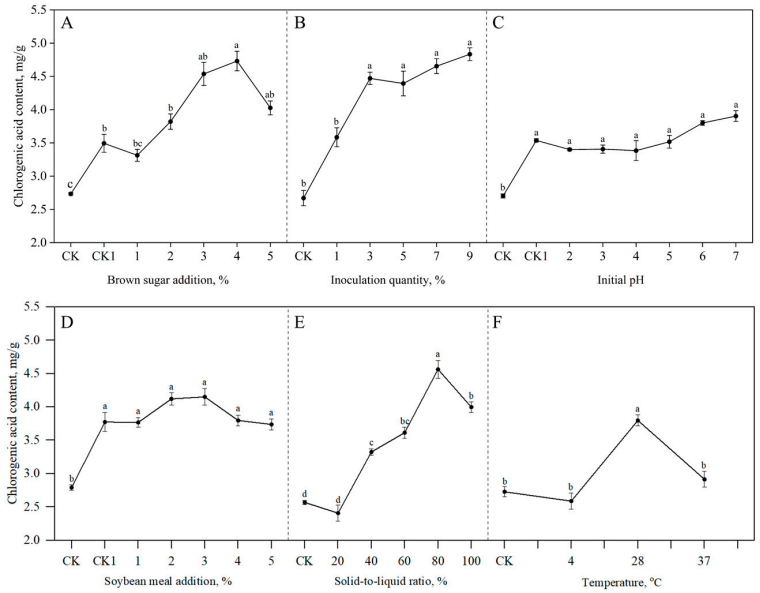


Figure 1. Effects of single-factor experiments on chlorogenic acid content for stevia residue fermentation. (**A**) Brown sugar addition; (**B**) inoculation quantity; (**C**) initial pH; (**D**) soybean meal addition; (**E**) solid-to-liquid ratio; (**F**) fermentation temperature. CK, stevia residue; CK1, fermented stevia residue without adding brown sugar, adjusting initial pH, or soybean meal addition. Significant differences ($p < 0.05$) among different groups are indicated by different lowercase letters.

Similarly, the effect of temperature on CA content showed a trend of initial increase followed by a decrease. The CA content reached its highest value (3.80 mg/g) at 28 °C. A temperature above or below 28 °C, however, caused a substantial decrease in CA content (Figure 1F).

Therefore, the temperature, solid-to-liquid ratio, and brown sugar addition were selected for a response surface optimization experiment.

3.2. Optimization of Fermented Stevia Residue Using Response Surface Optimization Experiment

The results of the RSM are presented in Tables 1 and 2. Based on the values for CA content (Y), the plotted response surfaces showed that three experimental parameters (A, B, and C) significantly influenced CA content. The corresponding regression equation is as follows:

Table 1. Response surface results of chlorogenic acid content.

Std	Run	Variables			Experimental
		A: Solid-to-Liquid Ratio, %	B: Brown Sugar Addition, %	C: Temperature, °C	Chlorogenic Acid Content, mg/g
1	5	60	1	28	4.59
2	15	100	1	28	3.34
3	11	60	5	28	3.43
4	4	100	5	28	4.10
5	9	60	3	4	3.25
6	10	100	3	4	2.56
7	8	60	3	37	3.90
8	12	100	3	37	4.04
9	3	80	1	4	2.86
10	14	80	5	4	3.00
11	6	80	1	37	3.89
12	17	80	5	37	3.83
13	16	80	3	28	4.83
14	13	80	3	28	4.77
15	2	80	3	28	4.73
16	7	80	3	28	4.94
17	1	80	3	28	4.93

Std, standard order; Run, run order.

Table 2. Analysis of variance of regression model equations.

SV	SDS	df	MS	F-Values	*p*-Values
Model	9.499	9	1.055	90.945	2.04×10^{-6}
A	0.242	1	0.242	20.883	2.575×10^{-3}
B	4.273×10^{-3}	1	4.273×10^{-3}	0.368	0.563
C	1.979	1	1.979	170.544	3.60×10^{-6}
AB	0.917	1	0.917	79.038	4.62×10^{-5}
AC	0.149	1	0.149	12.870	8.887×10^{-3}
BC	2.253×10^{-2}	1	2.253×10^{-2}	1.941	0.206
A^2	0.918	1	0.917	79.064	4.61×10^{-5}
B^2	1.087	1	1.087	93.645	2.66×10^{-5}
C^2	1.909	1	1.909	164.508	4.06×10^{-6}
Residual	8.124×10^{-2}	7	1.161×10^{-2}		
Lack of fit	4.585×10^{-2}	3	1.528×10^{-2}	1.728	0.299
Pure Error	3.538×10^{-2}	4	8.847×10^{-3}		
Cor Total	9.581	16			
R^2				0.992	
R^2 (Adj)				0.981	
CV%				2.731	

A, solid-to-liquid ratio; B, brown sugar addition; C, fermentation temperature; df, degree freedom; MS, mean square; SDS, standard deviation square.

$$Y = -1.38967 + 0.130286A - 0.163374B + 0.126631C + 0.011972AB + 0.000557AC - 0.002165BC - 0.001167A^2 - 0.127014B^2 - 0.003283C^2.$$

The analysis of variance (Table 2) for the regression model was significant (F = 90.945, $p < 0.001$), indicating a highly significant relationship between the independent variables and the response. The lack of fit term represented the degree of difference between the model used and the test. In this case, the *p*-value of 0.299 was beneficial to the model, suggesting a good fit and no lack of fit factor. Therefore, the regression equation accurately reflected the actual situation.

The regression equation was used to analyze the test results. The model showed an excellent fit, with a coefficient of determination (R^2) of 0.992, indicating that the model could explain 99.2% of the changes in the response value. The adjusted coefficient (R^2 Adj) was 0.981, and the coefficient of variation was 2.731%, suggesting that 1.9% of the variation in the model could not be explained by the model. Overall, the model fitted well and could be utilized to analyze and predict the CA content in FSR.

The F-value reflected the importance of each factor's influence on the test value. The one-order term coefficient of factors A and C had values of 0.130286 and 0.126631, respectively, both of which were positive values. The *p*-values of factors A and C were 2.575×10^{-3} and 3.60×10^{-6}, respectively, both of which were less than 0.05, indicating that the solid-to-liquid ratio and temperature had significant impacts on CA content. The binomial coefficients of factors A^2, B^2, and C^2 had values of −0.001167, −0.127014, and −0.003283, respectively, which were negative values. The *p*-values of A^2, B^2, and C^2 were less than 0.0001, indicating that A^2, B^2, and C^2 significantly influenced the CA content. On the other hand, the *p*-value of factor B ($p = 0.563$) was greater than 0.05, suggesting that factor B (brown sugar addition) did not have a significant impact on the CA content.

To further investigate the interactive effects of the solid-to-liquid ratio, brown sugar addition, and temperature on the CA content, contour and 3D response surface plots were analyzed (Figure 2). The RSM models provided an intuitive reflection of how pairs of factors influence the response value. In the 3D surface plots, a steeper slope indicated a stronger influence of that factor on the response value, while a smoother model suggested a weaker impact. Similarly, in the contour plots, a circular shape indicated a non-significant interaction between the two factors, whereas an elliptical shape suggested a significant interaction.

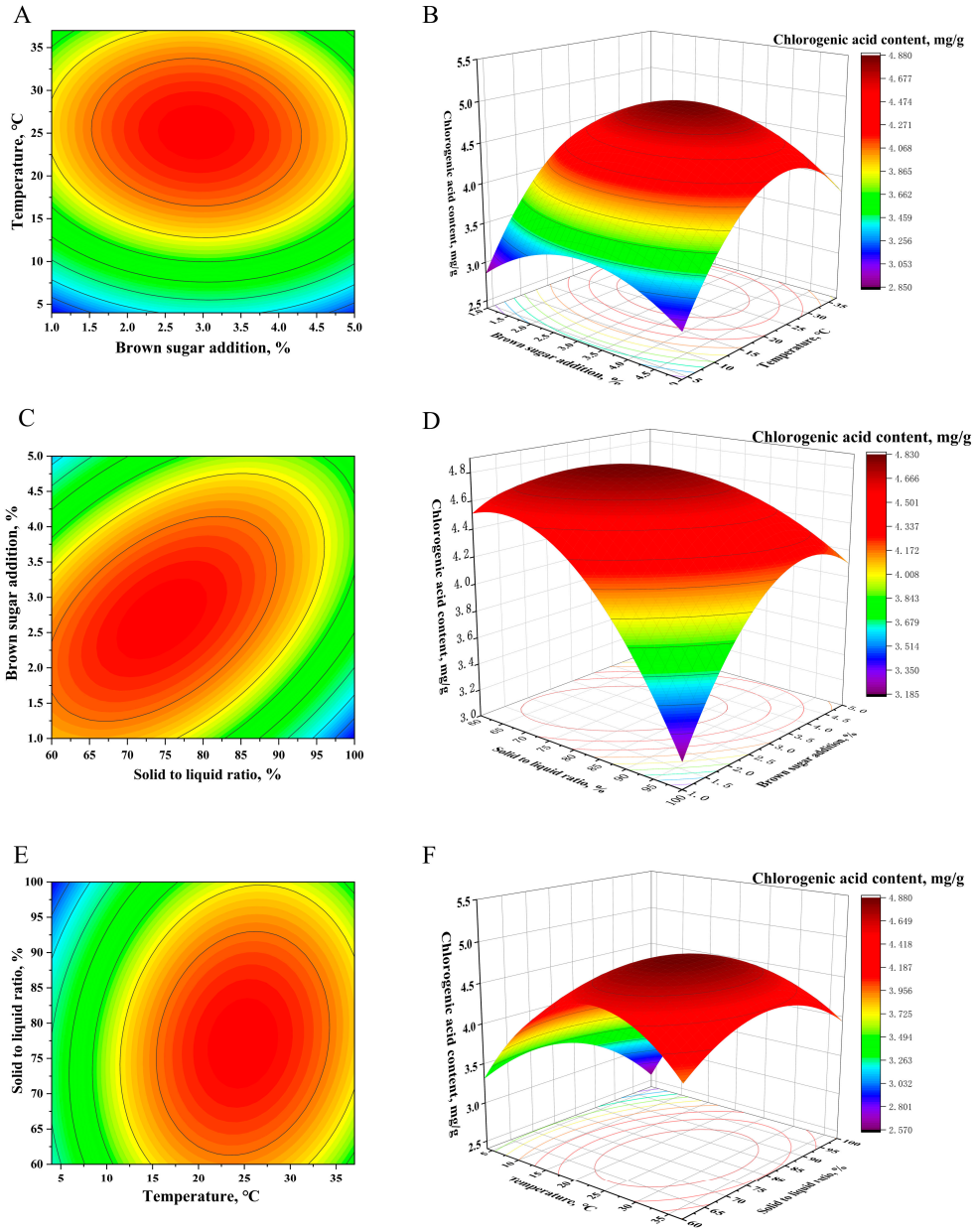


Figure 2. Response surface optimization process contours and response surface 3D maps. The contour (**A**) and response surface 3D maps (**B**) of the interaction between temperature and brown sugar addition; the contour (**C**) and response surface 3D maps (**D**) of the interaction between brown sugar addition and solid-to-liquid ratio; and the contour (**E**) and response surface 3D maps (**F**) of the interaction between temperature and solid-to-liquid ratio.

The RSM diagram revealed that the fermentation temperature had more pronounced effects on the CA content compared to brown sugar addition (Figure 2A). The results illustrated in Figure 2B indicate that the CA content in FSR initially increased and then decreased with the increase in fermentation temperature when the solid-to-liquid ratio was constant at 80%. The maximum CA content was observed at 25 °C. Similarly, the CA content exhibited an increasing trend, initially increasing and then decreasing with a gradual increase in brown sugar addition.

The RSM diagram revealed that the solid-to-liquid ratio had more pronounced effects on the CA content compared to brown sugar addition (Figure 2C). In Figure 2D, when the temperature was constant at 28 °C, the CA content in FSR initially increased and

then decreased when the brown sugar addition gradually increased. Similarly, as the solid-to-liquid ratio increased, the CA content initially increased and then decreased.

The RSM diagram revealed that the temperature surface changed more steeply compared to the solid-to-liquid ratio surface, indicating that temperature had a greater impact on CA content (Figure 2E). Figure 2F demonstrates that at a fixed 3% brown sugar addition, the CA content initially increased and then decreased with increasing fermentation temperature. Meanwhile, a similar increasing and decreasing pattern was observed with an increasing solid-to-liquid ratio.

Based on these findings, the optimal fermentation conditions to maximize CA (4.888 mg/g) content in SR were a solid-to-liquid ratio of 75.6%, brown sugar addition of 2.7%, and a fermentation temperature of 25 °C. For practical production, the following fermentation conditions were employed: inoculation quantity of 3%, brown sugar addition of 2.7%, solid-to-liquid ratio of 75%, temperature of 25 °C, and fermentation time of 9 days. Under these conditions, the CA content in the FSR was generally consistent with the theoretical value.

3.3. Fermented Stevia Residue Analysis Results

To further explore the changes in FSR after optimized fermentation, the physicochemical characteristics and functional active components were subsequently determined. The cell wall morphology of FSR is shown in Figure 3A. With increasing fermentation time, the cell wall of FSR, when fermented with the microbial agent and distilled water, showed an increasing trend of degradation. The cell wall degradation of FSR was more significant when fermented with a microbial agent compared with distilled water. These results indicated that the fermentation efficiency of FSR was superior with microbial agent fermentation than with distilled water fermentation.

As shown in Figure 3B, the cellulase activity in FSR was increased ($p < 0.05$) on days 3, 6, 9, 12, and 15 of fermentation. The cellulase activity showed a gradual increase first and then decreased, while it reached the highest value on day 12 of fermentation. Similarly, the laccase activity in FSR was increased ($p < 0.05$) on days 9, 12, and 15 of fermentation, showing a gradual upward trend that peaked on day 15 of fermentation.

As shown in Figure 3C,D, fermentation increased the content of soluble sugar, crude fat, and other nutrients in FSR but decreased the content of crude fiber ($p < 0.05$).

3.4. Metabolite Profile of Fermented Stevia Residue

A total of 594 metabolites were identified in all samples from FSR. The supervised partial least squares discriminant analysis (PLS-DA, Figure 4A) showed a distinct separation of the metabolites between SR and FSR. Based on the criteria of a *t*-test FDR < 0.05 and a VIP > 1, a total of 248 differential metabolites were identified in FSR. These metabolites included carboxylic acids and derivatives (47), fatty acyl (41), benzene and derivatives (29), organooxygen compounds (13), steroids and steroid derivatives (9), prenol lipids (9), flavonoids (8), phenols (8), indoles and derivatives (7), and others (77) (Figure 4B). KEGG enrichment analysis was performed to determine the metabolic pathways of these 248 differential metabolites. The results showed that these metabolites were significantly enriched in mainly phenylalanine/tyrosine/tryptophan biosynthesis, histidine metabolism, and phenylalanine metabolism (Figure 4C).

3.5. Microbiota Analysis of Fermented Stevia Residue

As shown in Figure 5A, compared with FSR on days 0–12, the Faith_pd index was increased ($p < 0.05$) in FSR on day 15 of fermentation, indicating an increase in bacterial diversity. Fermentation time had no significant effect ($p > 0.05$) on the Chao 1, Good's coverage, Observed_species, Pielou-evenness, Shannon, and Simpson indices.

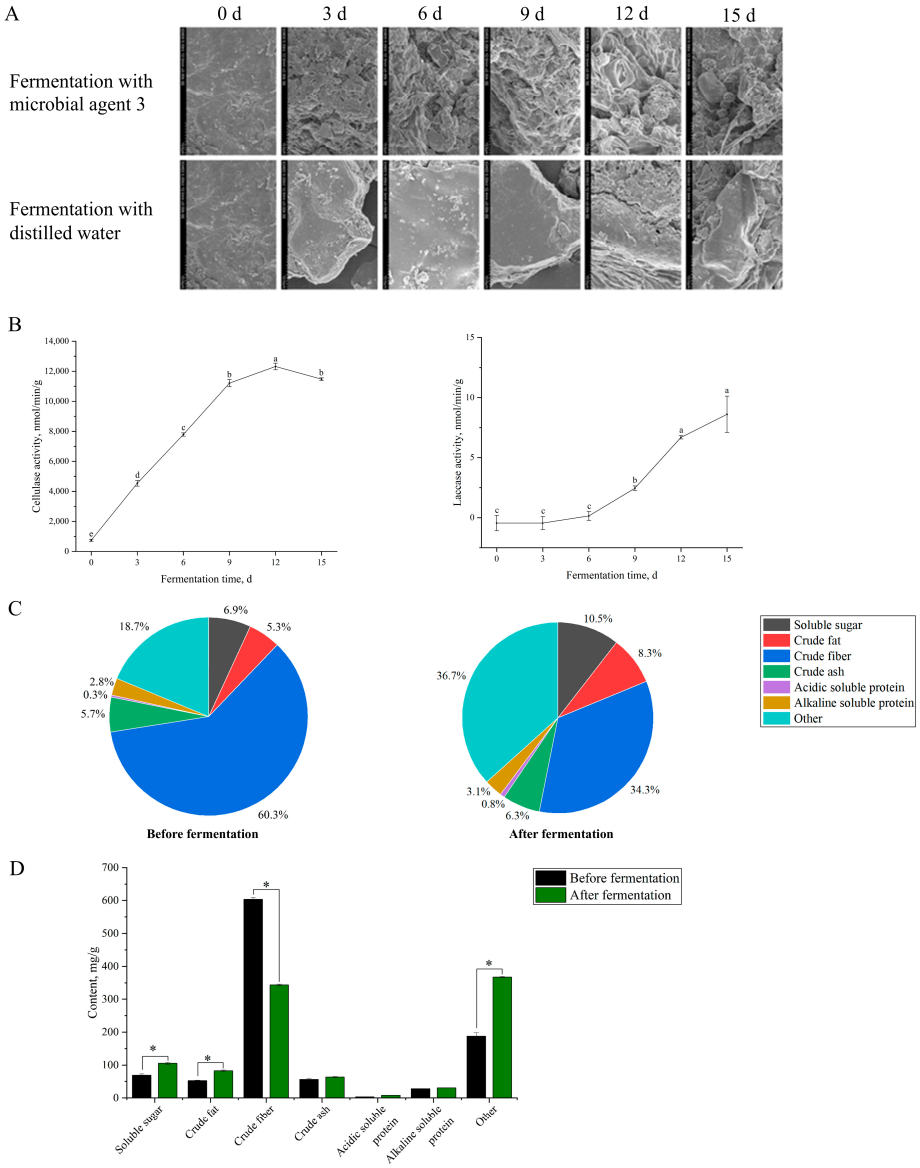


Figure 3. Characterization of fermented stevia residue: (**A**) Cell wall morphology observed by scanning electron microscopy, (**B**) activities of cellulase and laccase, (**C**) nutrient profile before and after fermentation, and (**D**) comparative analysis of nutrient content between before and after fermentation. Significant differences ($p < 0.05$) between means are indicated by different lowercase letters or *.

At the phylum level, *Proteobacteria*, *Firmicutes*, and *Deinococcota* were the most dominant phyla, followed by *Bacteroidota* and *Actinobacteriota* (Figure 5C). At the genus level, *Acinetobacter*, *Porphyrobacter*, *Deinococcus*, and *Enhydrobacter* were the most dominant genera, followed by *Brevundimonas*, *Sphingomonas*, and *Blastomonas* (Figure 5C). The Kruskal–Wallis test showed that no significant difference ($p > 0.05$) was found in bacterial communities at the phylum and genus levels at different fermentation stages.

To further identify the differences in bacterial communities in FSR at different fermentation stages, LEfSe analysis (LDA threshold ≥ 2) was performed at the genus level. The LEfSe analysis revealed that *Pseudomonas* was enriched in FSR on day 9 of fermentation, as well as *Franconibacter* and *Xylella* on day 12. On day 15 of fermentation, only *Pantoea* was enriched in FSR (Figure 5E,F).

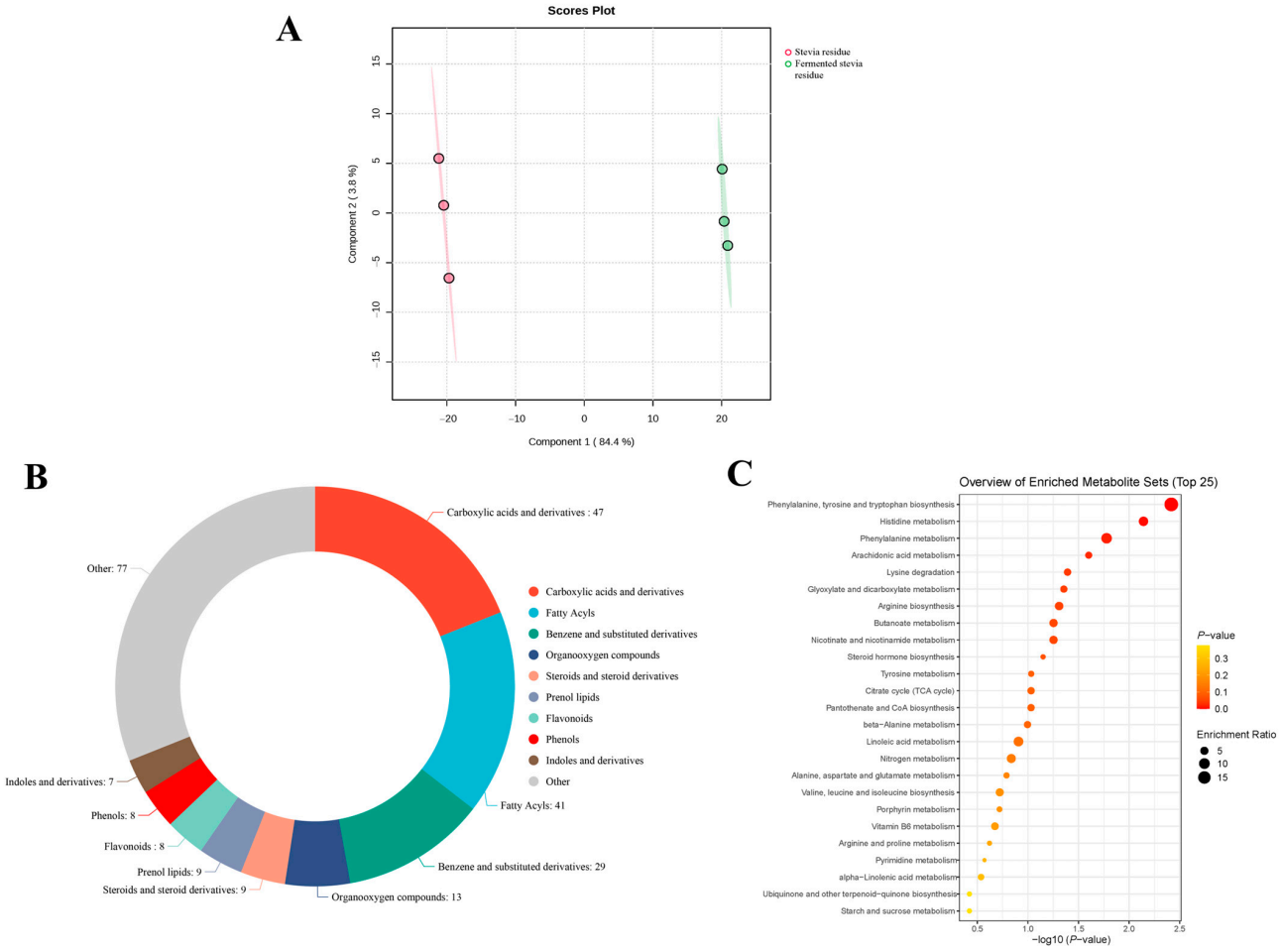


Figure 4. Metabolomics analysis. (**A**) Classification of differential metabolites; (**B**) PLS-DA score plot of metabolites; (**C**) KEGG pathway enrichment analysis of differential metabolites. $p < 0.05$ indicates that differential metabolites were significantly enriched in this pathway.

3.6. Mycobiome Analysis of Fermented Stevia Residue

As shown in Figure 6A, the Faith_pd index in FSR was increased ($p < 0.05$) on day 15 of fermentation compared with days 0–3. Fermentation time had no significant effect ($p > 0.05$) on the fungal Chao 1, Good's coverage, Observed_species, Pielou-evenness, Shannon, and Simpson indices.

At the phylum level, *Ascomycota* and *Phragmoplastophyta* were the most dominant phyla, followed by *Mucoromycota* and *Vertebrata*. The abundance of *Phragmoplastophyta* was higher on day 0 and subsequently decreased with fermentation time. Moreover, the abundances of *Mucoromycota* and *Vertebrata* showed an increasing trend first and then a decrease, with the maximum value attained on day 9 of fermentation. Meanwhile, the abundance of *Ascomycota* progressively increased throughout the fermentation, reaching its highest peak by day 15 of fermentation (Figure 6C).

At the genus level, the dominant genera were *Chaetomium*, *Pichia*, *Aspergillus*, and *Magnoliophyta*, followed by *Geotrichum*, *Cyberlindnera*, and *Mammalia*. The Kruskal–Wallis analysis revealed that *Chaetomium* displayed a higher abundance in FSR on day 15 than on days 0–12, whereas *Magnoliophyta* exhibited a higher abundance in FSR on day 0 than on days 12–15. Additionally, *Mammalia* displayed a higher abundance in FSR on day 9 than days on 0–6 and 12–15, whereas *Pichia* exhibited a higher abundance in FSR on day 15 than on days 0 and 6–12. *Trichoderma* displayed a higher abundance in FSR on days 12–15 than on days 0–9 (Figure 6D).

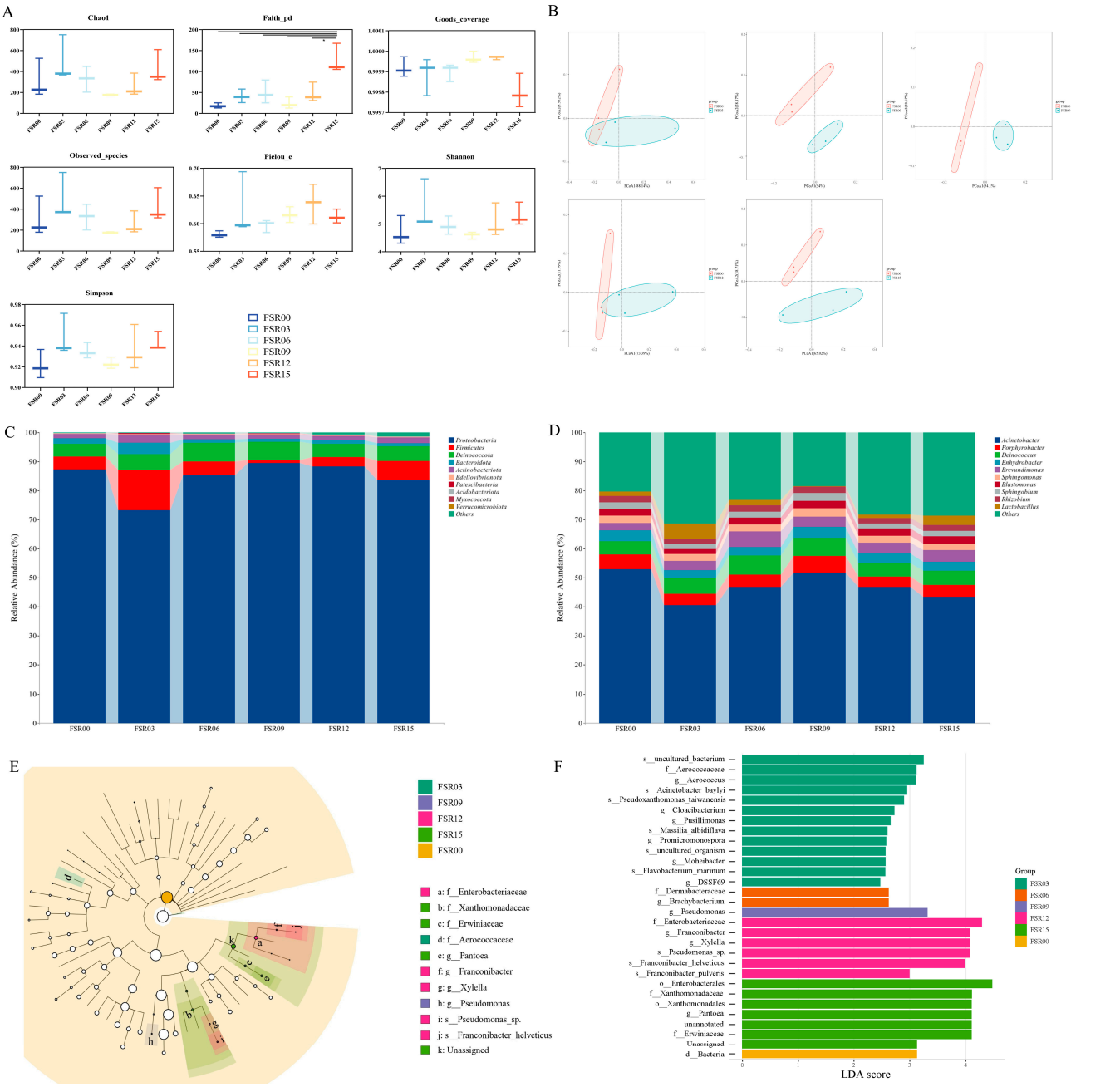


Figure 5. Effects of fermentation time on microbiota composition in fermented stevia residue (n = 3). (**A**) Alpha-diversity indices; (**B**) beta-diversity indices; (**C**) relative abundance of bacteria at the phylum level; (**D**) relative abundance of bacteria at the genus level; (**E**) taxonomic cladogram; (**F**) histogram of the distribution of LDA values for different bacteria identified by the LEfSe algorithm. Species with significant differences have an LDA score greater than the estimated score (2.0).

The LEfSe analysis revealed that *Magnoliophyta* was enriched in FSR on day 0 of fermentation. The abundance of *Cyberlindnera* was enriched in FSR on day 3, while *Flamella* was enriched in FSR on day 6 of fermentation. Only *Mammalia* was enriched in FSR on day 9 of fermentation. The abundances of *Chaetomium* and *Pichia* were enriched in FSR on day 15 of fermentation (Figure 6E,F).

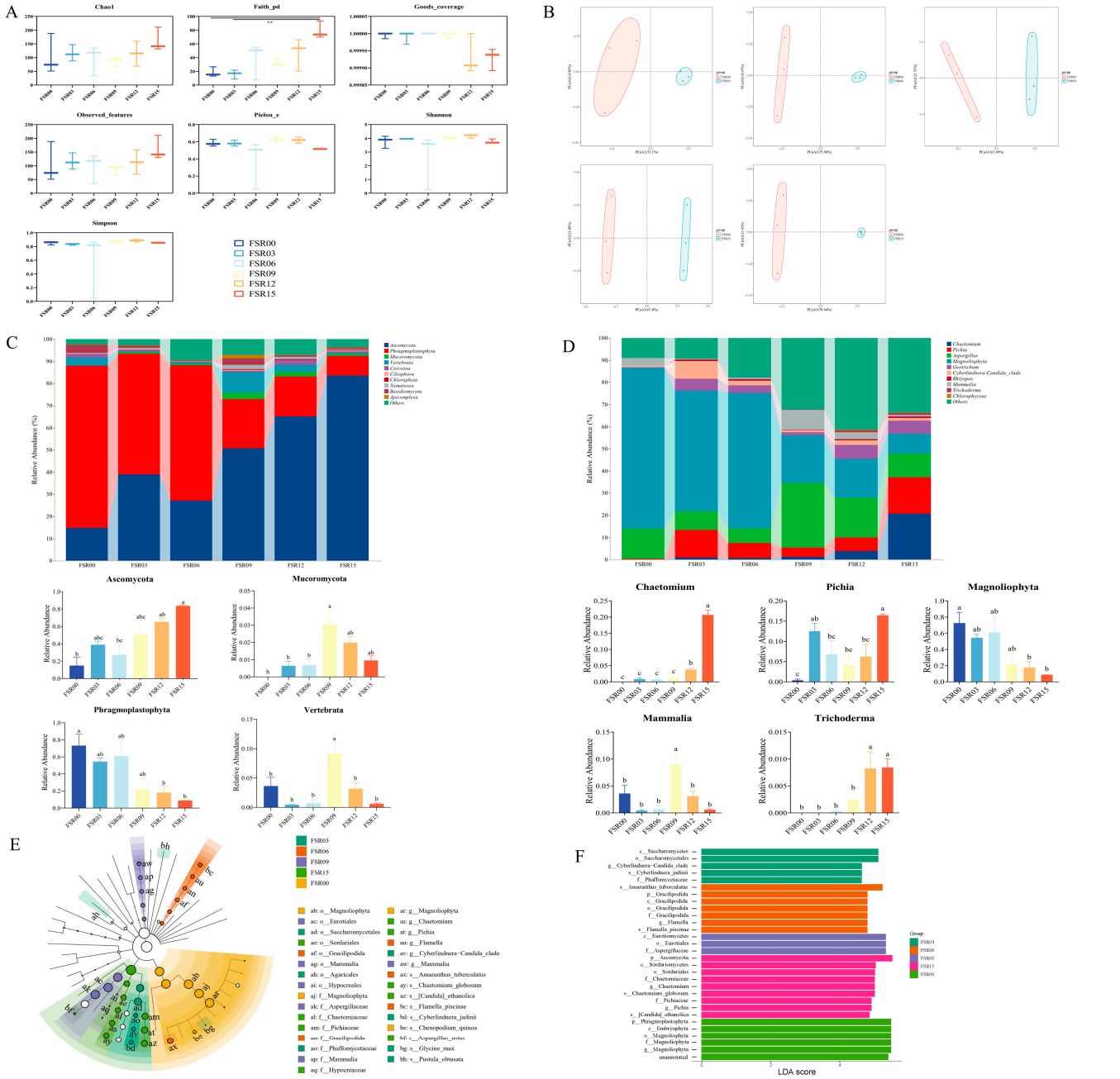


Figure 6. Effects of fermentation time on fungal composition of fermented stevia residue (n = 3): (**A**) Alpha-diversity indices; (**B**) beta-diversity indices; (**C**) composition and difference in relative abundance of fungi at the phylum level; (**D**) composition and difference in relative abundance of fungi at the genus level; (**E**) taxonomic cladogram; (**F**) histogram of the distribution of LDA values for different fungi identified by the LEfSe algorithm. Species with significant differences have an LDA score greater than the estimated score (2.0). Different lowercase superscript letters (a–c) indicate significant differences among different fermentation time ($p < 0.05$).

3.7. Effect of Fermented Stevia Residue on Production Performance of Laying Hens

Given the above findings that fermentation significantly enhanced the functional quality of SR, we further carried out an in vivo feeding trial in laying hens to verify its biological effects and establish a clear link between fermentation-induced improvements and laying hen physiology. As shown in Table 3, the AEW was higher ($p < 0.05$) in the 0.5% SR group compared with the 1.5% SR group, while the FER was lower ($p < 0.05$) compared with the 1.0–1.5% SR groups. Additionally, the ADFI was higher ($p < 0.05$) in

the control, 1.0–1.5% SR, and FSR groups compared with the 0.5% SR and FSR groups. These results suggest that low-dose supplementation relatively reduced feed intake, while moderate doses restored feed intake to normal levels. Regression analysis revealed that diet supplemented with SR had significant linear and quadratic effects on ALR ($p = 0.040$, linear model: $Y = -3.946X + 76.307$), AEW ($p = 0.039$, linear model: $Y = -0.742X + 51.030$; $p = 0.001$, quadratic model: $Y = -2.321X^2 + 2.739X + 50.450$), FER ($p = 0.004$, linear model: $Y = 0.210X + 2.488$), and ADFI ($p = 0.036$, linear model: $Y = 0.980X + 96.469$; $p = 0.017$, quadratic model: $1.901X^2 - 1.872X + 1.901$).

Table 3. Effects of dietary SR and FSR on the production performance of laying hens.

Items	Additive	Supplementation Doses (%)				SEM	*p*-Values		
		0	0.5	1.0	1.5		ANOVA	Linear	Quadratic
ADFI, g/hen/d	SR	97.33 ^{a}	95.32 ^{b}	98.14 ^{a}	98.03 ^{a}	0.264	<0.001	0.036	0.017
	FSR	97.33 ^{a}	95.65 ^{b}	97.92 ^{a}	97.96 ^{a}	0.262	0.002	0.076	0.087
AEW, g	SR	50.38 ^{ab}	51.44 ^{a}	50.66 ^{ab}	49.40 ^{b}	0.203	0.002	0.039	0.001
	FSR	50.38	50.15 *	50.76	50.75 *	0.175	0.559	0.279	0.752
ALR, %	SR	75.98	76.16	69.69	71.56	0.011	0.074	0.040	0.686
	FSR	75.98	74.20	74.38	69.96	0.011	0.264	0.071	0.547
FER	SR	2.56 ^{ab}	2.44 ^{b}	2.80 ^{a}	2.78 ^{a}	0.043	0.001	0.004	0.507
	FSR	2.56	2.59	2.60	2.78	0.040	0.182	0.050	0.336

Data are expressed as means with their SEM ($n = 8$). Different lowercase superscript letters (a and b) indicate significant differences among different supplemental doses of the same supplement (SR or FSR), while an asterisk (*) indicates a significant difference between the means of SR and FSR at the same dose level ($p < 0.05$). ADFI, average daily feed intake; ALR, average laying rate; AEW, average egg weight; FER, feed-to-egg ratio; FSR, fermented stevia residue; SR, stevia residue.

3.8. Effect of Fermented Stevia Residue on Egg Quality of Laying Hens

As shown in Table 4, the eggshell strength in the control, 1.0–1.5% SR, and FSR groups was lower ($p < 0.05$) compared with the 0.5% SR and FSR groups. Regression analysis revealed that diet supplemented with SR had significant linear effects on albumen height ($p = 0.019$, linear model: $Y = -0.713X + 5.102$), egg weight ($p = 0.019$, linear model: $Y = -3.477X + 55.735$), egg white percentage ($p = 0.022$, linear model: $Y = -0.026X + 0.578$), egg yolk percentage ($p = 0.033$, linear model: $Y = 0.017X + 0.298$), and eggshell percentage ($p = 0.025$, linear model: $Y = 0.006X + 0.129$). Additionally, diet supplemented with FSR had significant quadratic effects on egg white percentage ($p = 0.010$, quadratic model: $Y = 0.058X^2 - 0.090X + 0.576$) and egg yolk percentage ($p = 0.008$, quadratic model: $Y = -0.048X^2 + 0.073X + 0.295$). Diets supplemented with SR and FSR had no significant effect ($p > 0.05$) on egg yolk color, albumen height, Haugh unit, and egg shape index.

Table 4. Effects of dietary SR and FSR on egg quality of laying hens.

Items	Additive	Supplementation Doses (%)				SEM	*p*-Values		
		0	0.5	1.0	1.5		ANOVA	Linear	Quadratic
Albumen height, mm	SR	5.04	4.90	4.26	4.06	0.174	0.128	0.019	0.928
	FSR	5.04	4.80	4.50	4.59	0.187	0.758	0.327	0.671
Egg shape index	SR	1.33	1.35	1.34	1.34	0.005	0.580	0.477	0.431
	FSR	1.33	1.31 *	1.32	1.32	0.004	0.665	0.688	0.578
Egg white percentage, %	SR	57.84	56.55	54.89	54.13	0.006	0.159	0.022	0.827
	FSR	57.84	53.94	54.99	56.87 *	0.006	0.055	0.723	0.010
Egg yolk color	SR	13.58	13.38	13.50	13.10	0.118	0.517	0.217	0.694
	FSR	13.58	13.83	13.75	13.23	0.118	0.284	0.284	0.102

Table 4. *Cont.*

Items	Additive	Supplementation Doses (%)				SEM	*p*-Values		
		0	0.5	1.0	1.5		ANOVA	Linear	Quadratic
Egg yolk percentage, %	SR	29.43	31.20	31.61	32.09	0.004	0.165	0.033	0.451
	FSR	29.43	32.26	31.69	29.71 *	0.005	0.060	0.949	0.008
Eggshell percentage, %	SR	12.74	13.56	13.50	13.78	0.002	0.088	0.025	0.368
	FSR	12.74	13.80	13.33	13.42	0.002	0.090	0.251	0.109
Eggshell strength, N	SR	41.99 ^{a}	37.18 ^{b}	39.62 ^{ab}	37.89 ^{ab}	0.619	0.021	0.074	0.202
	FSR	41.99 ^{a}	35.40 ^{b}	42.43 ^{a}	40.26 ^{ab}	0.817	0.004	0.805	0.187
Eggshell thickness, mm	SR	0.34	0.33	0.34	0.35	0.003	0.254	0.323	0.185
	FSR	0.34	0.31	0.34	0.34	0.005	0.070	0.637	0.111
Haugh unit	SR	66.15	67.79	63.31	61.92	1.586	0.569	0.232	0.639
	FSR	66.15	67.41	65.45	65.74	1.657	0.979	0.833	0.889

Data are expressed as means with their SEM (n = 8). Different lowercase superscript letters (a and b) indicate significant differences among different supplemental doses of the same supplement (SR or FSR), while an asterisk (*) indicates a significant difference between the means of SR and FSR at the same dose level ($p < 0.05$). FSR, fermented stevia residue; SR, stevia residue.

3.9. Effects of Fermented Stevia Residue on Plasma Antioxidant Capacity and Immune Function of Laying Hens

As shown in Table 5, the T-AOC capacity level was increased ($p < 0.05$) in all treatment groups regardless of SR and FSR doses, as well as the MDA concentration in the 0.5% SR group, when compared with the control group. The MDA concentration in the 0.5–1.0% FSR groups was decreased ($p < 0.05$) compared with the 1.5% FSR group. The increased T-AOC and decreased MDA indicate that both SR and FSR effectively enhanced the antioxidant status of laying hens, and FSR exhibited better effects. Regression analysis revealed that diet supplemented with SR had significant linear and quadratic effects on MDA concentration ($p = 0.048$, quadratic model: $Y = -0.255X^2 + 0.441X + 0.424$) and T-AOC capacity level ($p < 0.001$, linear model: $Y = 0.107X + 0.275$; $p < 0.001$, quadratic model: $Y = -0.171X^2 + 0.364X + 0.233$). Additionally, diets supplemented with FSR had significant quadratic effects on MDA concentration ($p < 0.001$, quadratic model: $Y = 0.368X^2 - 0.512X + 0.404$) and T-AOC capacity level ($p < 0.001$, linear model: $Y = 0.123X + 0.267$; $p < 0.001$, quadratic model: $Y = -0.162X^2 + 0.366X + 0.227$). Diets supplemented with SR or FSR had no significant effect ($p > 0.05$) on GSH-PX activity.

As shown in Table 5, the plasma IgA concentration in the 1.0–1.5% SR and 1.5% FSR groups was higher ($p < 0.05$) compared with the control group, while plasma IgY concentration was higher ($p < 0.05$) in the 1.0% SR group compared with the control and 1.5% SR groups. These results demonstrate that moderate and high doses of SR and FSR significantly enhanced immune function in laying hens. Regression analysis revealed that diet supplemented with SR had significant linear and quadratic effects on the concentrations of IgA ($p < 0.001$, linear model: $Y = 1786.571X + 5339.000$; $p = 0.016$, quadratic model: $Y = -1858.571X^2 + 4574.429X + 4874.357$) and IgY ($p = 0.010$, quadratic model: $Y = -2885.099X^2 + 4044.345X + 7898.294$). Additionally, diets supplemented with FSR had significant linear and quadratic effects on the concentrations of IgA ($p = 0.001$, linear model: $Y = 2055.714X + 4930.000$) and IgY ($p = 0.027$, quadratic model: $Y = 1867.146 X^2 - 3253.142X + 8249.551$).

Table 5. Effects of dietary SR and FSR on plasma antioxidant capacity and immune function in laying hens.

Items	Additive	Supplementation Doses (%)				SEM	*p*-Values		
		0	0.5	1.0	1.5		ANOVA	Linear	Quadratic
GSH-PX, U/mL	SR	285.25	280.85	271.94	277.67	2.247	0.201	0.118	0.251
	FSR	285.25	286.63	278.30	278.24	2.547	0.546	0.206	0.890
MDA, nmol/mL	SR	0.40 ^{b}	0.65 ^{a}	0.54 ^{ab}	0.53 ^{ab}	0.033	0.044	0.353	0.048
	FSR	0.40 ^{ab}	0.24 ^{b*}	0.26 ^{b*}	0.46 ^{a*}	0.032	0.006	0.527	<0.001
T-AOC, nmol Trolox/mL	SR	0.22 ^{b}	0.41 ^{a}	0.38 ^{a}	0.41 ^{a}	0.019	<0.001	<0.001	<0.001
	FSR	0.22 ^{b}	0.39 ^{a}	0.41 ^{a}	0.42 ^{a}	0.020	<0.001	<0.001	<0.001
IC Ab, pg/mL	SR	202.58	189.85	195.64	199.18	2.590	0.369	0.855	0.129
	FSR	202.58	200.30	205.73	200.58	2.208	0.836	0.978	0.761
IgA, ng/mL	SR	5037.14 ^{c}	6208.57 ^{bc}	8078.57 ^{a}	7391.43 ^{ab}	301.542	<0.001	<0.001	0.016
	FSR	5037.14 ^{b}	6522.86 ^{b}	5534.29 ^{b*}	8792.86 ^{a}	378.843	<0.001	0.001	0.115
IgM, ng/mL	SR	5686.67	5093.33	5114.44	5276.67	182.218	0.670	0.473	0.320
	FSR	5686.67	5688.89	5523.33	5517.78	193.139	0.983	0.708	0.992
IgY, ng/mL	SR	8163.38 ^{b}	8403.95 ^{ab}	9852.78 ^{a}	7208.26 ^{b}	288.914	0.003	0.597	0.010
	FSR	8163.38	7348.29	6605.03 *	7657.09	219.592	0.070	0.260	0.027

Data are expressed as means with their SEM (n = 5). Different lowercase superscript letters (a–c) indicate significant differences among different supplemental doses of the same supplement (SR or FSR), while an asterisk (*) indicates a significant difference between the means of SR and FSR at the same dose level ($p < 0.05$). GSH-PX, glutathione peroxidase; FSR, fermented stevia residue; IC Ab, chicken infectious coryza antibody; IgA, immunoglobulin A; IgM, immunoglobulin M; IgY, immunoglobulin Y; MDA, malondialdehyde; SR, stevia residue; T-AOC, total antioxidant capacity.

4. Discussion

This study systematically integrates fermentation optimization, compositional changes, microbial succession, metabolite alterations, and in vivo performance into a unified interpretation. Microbial fermentation is widely employed to improve the nutritional composition and enhance the utilization efficiency of agricultural by-products. Multiple interacting factors govern the success of this process. For instance, inoculant quantity strongly impacts both microbial growth and substrate conversion efficiency [23], while both initial pH and soybean meal addition are closely associated with the quality and quantity of fermentation products [24,25]. Consistently, our single-factor experiments identified brown sugar addition, inoculation quantity, pH, soybean meal addition, solid-to-liquid ratio, and temperature as significant influencers of CA content in FSR. The underlying mechanisms for these observations are multifaceted. The CA content in FSR increased with brown sugar addition, which may be attributed to the fact that brown sugar can facilitate microbial growth and fermentation efficiency by supplying essential nutrients through its organic compounds and regulating pH to establish an optimal environment [26]. Similarly, the solid-to-liquid ratio was critical, as an excessively low solid-to-liquid ratio limits sufficient contact between SR and the solvent, thereby reducing fermentation efficiency [27]. Temperature also played a pivotal role in fermentation efficiency. In this study, the CA content reached its highest value at 28 °C, which presumably facilitated optimal enzymatic reactions and microbial activity [28]. In contrast, deviations from this temperature hindered microbial community growth and reproduction, compromising fermentation efficiency and ultimately leading to a decrease in CA content in FSR. Our findings underscore that CA production in FSR is modulated by a complex interplay of nutritional, physical, and chemical factors. Therefore, selecting optimal fermentation conditions requires a holistic approach that integrates the results of single-factor and response surface experiments, balancing fermentation efficiency with the stability of raw materials.

Cellulose and lignin, the key structural components of the plant cell wall, are degraded by specific microbial hydrolytic enzymes, including cellulase and laccase [29]. In this study, cellulase activity initially increased and then decreased, reaching its highest value on day

12 of fermentation. Similarly, laccase activity in FSR was increased on days 9, 12, and 15 of fermentation, showing a gradual upward trend that peaked on day 15 of fermentation. These findings indicated that the fermentation efficiency of SR was significantly enhanced during the later fermentation stage. Consistent with these findings, the nutritional profile in FSR was altered accordingly: soluble sugar and crude fat content increased, while crude fiber content decreased. This may be attributed to the enhanced cellulase activity in the late fermentation stage, as cellulase can hydrolyze cellulose into glucose and other hydrolysis products [30].

Flavonoids, benzene derivatives, and other substances enriched in FSR are well-known natural antioxidants [31], while carboxylic acids (such as short-chain fatty acids, SCFAs) and indole derivatives play a key role in intestinal health [32]. In this study, metabolomic analysis revealed that a variety of differential metabolites, including flavonoids, phenols, indoles, and their derivatives, were significantly enriched in FSR. These metabolites might be associated with the improved antioxidant and immune effects of FSR. These findings suggest that microbial fermentation significantly reshaped the metabolite profile of FSR, converting it from a simple fibrous feedstock into a complex functional material enriched with bioactive molecules.

Bacterial diversity reflects the complexity of microbes in terms of species, numbers, and functional activities. Key bacterial genera, including *Pseudomonas*, *Pantoea*, *Franconibacter*, and *Xylella*, were identified as dominant functional taxa contributing to substrate decomposition and metabolite synthesis during fermentation. In this study, compared with FSR on days 0–12, the Faith_pd index was higher in FSR on day 15 of fermentation, indicating increased bacterial diversity. The increased bacterial diversity indicates that the microecological structure of the fermentation system was more stable, with enhanced organic acid metabolism and antibacterial activity, which was conducive to improving safety and palatability. *Pseudomonas* can secrete various hydrolases and effectively decompose macromolecules such as proteins and lipids, thereby laying a foundation for subsequent fermentation [33]. The LEfSe analysis revealed that *Pseudomonas* was enriched in FSR on day 9 of fermentation, as well as *Franconibacter* and *Xylella* on day 12. Thus, the enrichment of *Pseudomonas* may be related to the requirement of the fermentation system for rapid degradation of complex organic compounds. Additionally, the enrichment of *Franconibacter* and *Xylella* may be attributed to the suitable ecological niche created by organic acids or oligopeptides generated from the degradation of organic matter in the early stage. *Pantoea* can utilize a variety of monosaccharides and organic acids and exerts significant beneficial effects on plant growth [34]. On day 15 of fermentation, only *Pantoea* was enriched in FSR, which may reflect the relatively abundant presence of soluble sugars and other degradation products of cellulose and hemicellulose in the fermentation system. These findings indicated that the bacterial community in FSR underwent succession during fermentation.

Similarly, the Faith_pd index in FSR was higher on day 15 compared with days 0–3 of fermentation, suggesting a significant expansion in the phylogenetic diversity of the fungal community of FSR. The increased fungal diversity suggests that complex carbohydrates such as cellulose and hemicellulose in SR were more completely degraded, fermentation depth was improved, and feed digestibility was enhanced.

At the phylum level, *Ascomycota* and *Phragmoplastophyta* were the most dominant phyla, followed by *Mucoromycota* and *Vertebrata*. *Phragmoplastophyta* is a plant division comprising multicellular charophytes and land plants [35]. A previous study has reported that *Phragmites karka*, a member of *Phragmoplastophyta*, can be saccharified by bacterial enzymes to provide carbon sources for microbial fermentation [36]. Additionally, as a decomposer of many plant materials [37], *Mucoromycota* were found to utilize sucrose as a carbon source for their metabolic activities [38]. In the present study, the abundance of *Phragmoplastophyta* was higher on day 0 of fermentation and subsequently decreased with

fermentation time. Moreover, the abundance of *Mucoromycota* showed an initial increase followed by a decrease, with the maximum value observed on day 9 of fermentation. It is hypothesized that organic matter produced by the early-stage activities of *Phragmoplastophyta*, along with the added brown sugar, serves as a carbon source for the metabolic activities of *Mucoromycota*. Meanwhile, *Ascomycota*, represented by taxa such as *Aspergillus*, *Penicillium*, *Chaetomium*, and *yeasts* [39], progressively increased in relative abundance throughout the fermentation period, reaching a peak on day 15. We hypothesized that the early-stage *Mucoromycota* activity modified the fermentation substrate, thereby facilitating the subsequent proliferation of *Ascomycota*. This alteration in microbial communities during fermentation demonstrated the transformation and purification of the substrate, indicating the effectiveness of the fermentation process.

At the genus level, the dominant fungal genera were *Chaetomium*, *Pichia*, *Aspergillus*, and *Magnoliophyta*, followed by *Geotrichum*, *Cyberlindnera*, and *Mammalia*. Among these fungi, key fungal genera, including *Chaetomium*, *Pichia*, and *Trichoderma*, are known as the core functional fungi that contribute to fiber degradation and functional metabolite production. *Chaetomium*, a saprophytic ascomycete fungus, is known to produce cellulase and hemicellulase [40]. Similarly, *Trichoderma*, a ubiquitous filamentous ascomycete fungus, produces cellulase and laccase [41]. In the present study, *Chaetomium* and *Trichoderma* abundances were increased during the later stages of fermentation (days 12–15). This temporal pattern is associated with the peak enzymatic activities of cellulase and laccase observed in the same period. Consequently, these findings indicate that the fermentation system had reached a stage characterized by efficient fiber and lignin degradation, which in turn contributed to the overall fermentation efficiency and product quality. *Pichia*, a probiotic yeast, also increased in abundance during the later fermentation phase. This was consistent with a previous study, which reported that *Pichia* was a dominant member of the microbiota during pickle fermentation [42]. The proliferation of *Pichia* was likely attributable to its utilization of oligosaccharides and organic acids generated by prior microbial degradation. Additionally, the decline in the abundances of *Mammalia* and *Phragmoplastophyta* collectively indicated the successful establishment of fermentative microbes and the efficient conversion of raw SR during the fermentation process.

The LEfSe analysis revealed that *Magnoliophyta* was enriched in FSR on day 0 of fermentation. The abundance of Cyberlindnera was enriched in FSR on day 3 of fermentation, while *Flamella* was enriched in FSR on day 6. Only *Mammalia* was enriched in FSR on day 9 of fermentation. The abundances of *Chaetomium* and *Pichia* were enriched in FSR on day 15 of fermentation. These findings indicated that the fungal community underwent a directed and orchestrated succession. This succession pattern collectively facilitated the decomposition and transformation of cellulose and lignin, indicating that the final FSR may possess improved flavor profiles and bioactivity.

Sustaining superior laying performance is of great importance for the economic development of the laying hen industry. In this study, ADFI displayed a biphasic trend: it was reduced at the 0.5% SR and FSR inclusion level but recovered and even increased at higher levels (1.0–1.5% SR and FSR). This change was biologically meaningful and reflected the adaptation of laying hens to dietary components. The initial reduction in ADFI may reflect dietary transition stress, whereas the subsequent recovery is consistent with improved palatability due to cell wall degradation and increased soluble sugars and fat, thereby promoting higher feed consumption. Furthermore, the natural sweeteners, such as steviol glycosides, present in SR also contributed to promoting feed intake [43]. Taking together, dietary inclusion levels of 1.0–1.5% were found to be optimal for maximizing production performance in laying hens.

As an important indicator for quantitatively evaluating the freshness and nutritional safety of eggs, egg quality is of great significance for ensuring food safety and eating quality for consumers. In this study, the decreasing trends in eggshell strength in the 0.5% SR and FSR groups indicated that low-dose supplementation with SR and FSR impaired egg quality in laying hens. This decline in eggshell strength may be associated with the crude fiber and anti-nutritional factors introduced by low-dose addition [44], which may impair intestinal microbial community structure and interfere with nutrient metabolism [45], while the beneficial biological functions of SR and FSR were not sufficiently activated to counteract the adverse effects. Additionally, eggs have extremely high nutritional value. The egg yolk is rich in nutrients such as vitamins, minerals, and fatty acids, but it also contains high levels of cholesterol and fat [46]. Moreover, the egg white provides high-quality protein with the least amount of fat or cholesterol [46]. In this study, the *t*-test showed that the 1.5% FSR group had a higher egg white ratio and a lower egg yolk ratio compared to the 1.5% SR group. These results indicated that FSR had better effects than SR, and supplementation with 1.0–1.5% FSR increased the protein content in eggs. Such egg products are highly suitable for fitness enthusiasts who require high protein intake for muscle building and fat reduction.

The key metabolites and functional microorganisms identified above acted synergistically to enhance antioxidant capacity and immune function in laying hens. The activities of T-AOC and GSH-Px serve as important indicators for assessing the antioxidant capacity of hens [47]. In this study, the T-AOC level was increased in all treatment groups, regardless of SR and FSR doses, compared with the control group. Firstly, CA was identified as the primary functional component, while other bioactive substances in FSR, such as flavonoids and benzene derivatives, also served as important bioactive constituents. These compounds can be absorbed through the intestinal tract and potentially clear excessive free radicals in the body, thereby enhancing the antioxidant capacity, which could lead to the enhanced T-AOC level observed in the plasma of laying hens [48]. Subsequently, bacterial species, including *Streptomyces*, *Nocardia*, and *Rhodococcus*, have been reported to degrade lignin by secreting peroxidases [49]. This process may generate small molecules with antioxidant activity, which could be another reason for enhanced antioxidant capacity. In addition, the biosynthetic pathways of phenylalanine, tyrosine, and tryptophan are closely linked to antioxidant capacity [50]. Specifically, tryptophan serves as a precursor for the synthesis of both the neurotransmitter serotonin and vitamin B_3 (niacin) [51], both of which are recognized as significant antioxidants. Meanwhile, tyrosine is the direct precursor to melanin, a potential biological antioxidant that effectively quenches free radicals [52]. Consistent with our metabolomics findings, the significant enrichment of amino acid metabolic pathways in the FSR group, particularly the elevated levels of key precursors such as tryptophan and tyrosine, provides a potential explanation for the increased plasma T-AOC capacity level and decreased MDA concentration in laying hens. Additionally, the *t*-test showed that the MDA concentration in the SR groups was significantly higher than in the FSR groups, indicating that the enhancement of antioxidant capacity in laying hens by FSR was greater than that induced by SR. In summary, 0.5–1.0% FSR was considered the optimal dose for enhancing antioxidant capacity in laying hens. It should be noted that the above interpretations are based on correlative evidence; therefore, direct causal relationships between specific metabolites, microbial taxa, and antioxidant responses need to be verified by further targeted mechanistic studies.

The immune function of laying hens plays a critical role in maintaining physiological homeostasis, disease resistance, and sustainable production performance. In agreement with the changes in microbial community structure and differential metabolites caused by solid-state fermentation, dietary FSR supplementation exerted comprehensive immunomodulatory effects on laying hens. In this study, the plasma IgA concentration in

the 1.0–1.5% SR and 1.5% FSR groups was higher compared with the control group, while plasma IgY concentration was higher in the 1.0% SR group compared with the control and 1.5% SR groups. The improved immune function was mainly attributed to CA and key functional metabolites such as SCFAs. The carboxylic acids enriched in FSR, such as SCFAs, can regulate the activity of immune cells, thereby promoting the synthesis and secretion of immunoglobulins, which is likely the reason for the enhanced immune function in laying hens [53]. Additionally, amino acid metabolism is fundamental to immune function, as it regulates both innate and adaptive responses through mechanisms such as immune cell activation and antibody production [54]. Specifically, the histidine pathway and its metabolite histamine serve as key immunomodulatory agents [55]. Similarly, tryptophan metabolism plays a central role in mediating immune tolerance and modulating inflammatory responses [56]. The metabolomics data in the present study also reveal amino acid metabolic reprogramming, suggesting that the fermented product could directly influence the immune function of laying hens by supplying immunologically active amino acids, such as tryptophan and histidine. This finding aligns with our observed increase in plasma immunoglobulins (e.g., IgY and IgA), collectively suggesting that dietary FSR enhances the host's humoral immune response via a nutri-immunological pathway.

Furthermore, as reflected in the microbiota results, *Pichia* not only inhibits the growth of pathogenic microorganisms [57] but also produces nutrients and flavor compounds that enhance the sensory characteristics and overall worth of the fermentation product [58]. It may be hypothesized that, following ingestion by laying hens, *Pichia* could exert sustained probiotic activity in the intestinal environment, which might partially account for the observed improvements in immune and antioxidant functions. However, since gut microbiota data from the laying hens were not analyzed in the present study, direct in vivo evidence supporting this mechanism is lacking. Therefore, the increased abundance of *Pichia* observed during *in vitro* fermentation provides only a potential explanation for the enhanced immune performance. These *in vitro* findings cannot be regarded as definitive proof of the underlying *in vivo* physiological pathways, and further investigation is warranted. Although the *t*-test indicated that the concentrations of IgA and IgY in the 1.0% SR group were significantly higher than those in the 1.0% FSR group, both the SR and FSR groups showed an upward trend in IgA and IgY concentrations compared with the control group. These findings suggested that supplementation with either SR or FSR improved immune performance in some contexts. Collectively, 1.0–1.5% FSR doses were identified as optimal for improving the immune performance of laying hens.

However, the main limitation of the present study was the duration of the feeding period. Although a 28-day feeding period was sufficient to reflect the short-term effects of FSR on laying hens, this duration may be relatively limited for assessing the persistent and stable responses in production performance and egg quality of 50-week-old laying hens. Therefore, future studies for a longer feeding period (8–12 weeks) are warranted to further verify the long-term efficacy and stability of FSR used as a feed additive.

5. Conclusions

The current study established an optimized fermentation process for SR, with the optimum conditions being a solid-to-liquid ratio of 75%, inoculation quantity of 3%, brown sugar addition of 2.7%, a temperature of 25 °C, and a fermentation period of 9 days. This process achieved a high CA content of 4.888 mg/g. The application of SR and FSR in laying hen diets revealed that the FSR supplementation improved average daily feed intake, antioxidant capacity, and immune performance. Considering production performance, egg quality, antioxidant capacity, and immune performance, the optimal supplementary dose of FSR under the experimental conditions of this study was determined to be 1.0%. Therefore,

fermentation effectively enhanced the bioactivity of SR, positioning it as a valuable additive for sustainable poultry production.

Supplementary Materials: The following supporting information can be downloaded at: https://www.mdpi.com/article/10.3390/agriculture16091009/s1, Table S1: Single-factor experiment design for stevia residue fermentation; Table S2: Response surface optimization experiment design for stevia residue fermentation; Table S3: Composition and nutrient levels of the basal diet (%, as-fed basis).

Author Contributions: F.H.: Data Curation, Formal Analysis, Investigation, Methodology, Writing—Original Draft, Writing—Review and Editing. B.Q.: Data Curation, Formal Analysis, Writing—Original Draft, Writing—Review and Editing. Y.W.: Data Curation, Formal Analysis, Investigation, Methodology. M.A.K.A.: Writing—Original Draft, Writing—Review and Editing. Y.F.: Writing—Original Draft, Writing—Review and Editing. X.K.: Conceptualization, Funding Acquisition, Project Administration, Resource, Supervision, Writing—original Draft, Writing—Review and Editing. F.L.: Conceptualization, Project Administration, Resource, Supervision, Writing—Original Draft, Writing—Review and Editing. All authors have read and agreed to the published version of the manuscript.

Funding: This research was jointly supported by the City-School Cooperation Project of the Special Funds of Science and Technology in Fuyang City undertaken by Fuyang Normal University (SXHZ2020007), and the Sub-project of the Central Government Guidance Fund for Local Science and Technology Development (ZY23CG44-1).

Institutional Review Board Statement: The animal experiments were reviewed and approved by the protocol management and review committee of the Institute of Subtropical Agriculture, Chinese Academy of Sciences (No. ISA-2022-056, approved on 15 March 2022).

Data Availability Statement: The data presented in this study are openly available in the Science Data Bank at https://www.scidb.cn/s/fUFZJr (accessed on 24 February 2026).

Conflicts of Interest: The authors declare no conflicts of interest.

References

1. Alagawany, M.; Elnesr, S.S.; Farag, M.R.; Abd El-Hack, M.E.; Barkat, R.A.; Gabr, A.A.; Foda, M.A.; Noreldin, A.E.; Khafaga, A.F.; El-Sabrout, K.; et al. Potential role of important nutraceuticals in poultry performance and health—A comprehensive review. *Res. Vet. Sci.* **2021**, *137*, 9–29. [CrossRef]
2. Nm, J.; Joseph, A.; Maliakel, B.; Im, K. Dietary addition of a standardized extract of turmeric (TurmaFEED(TM)) improves growth performance and carcass quality of broilers. *J. Anim. Sci. Technol.* **2018**, *60*, 8. [CrossRef] [PubMed]
3. Kothari, D.; Lee, W.D.; Niu, K.M.; Kim, S.K. The genus *Allium* as poultry feed additive: A review. *Animals* **2019**, *9*, 1032. [CrossRef]
4. Sheoran, N.; Kumar, R.; Kumar, A.; Batra, K.; Sihag, S.; Maan, S.; Maan, N.S. Nutrigenomic evaluation of garlic (*Allium sativum*) and holy basil (*Ocimum sanctum*) leaf powder supplementation on growth performance and immune characteristics in broilers. *Vet. World* **2017**, *10*, 121–129. [CrossRef]
5. Ashwell, M. Stevia, nature's zero-calorie sustainable sweetener: A new player in the fight against obesity. *Nutr. Today* **2015**, *50*, 129–134. [CrossRef] [PubMed]
6. Karaköse, H.; Jaiswal, R.; Kuhnert, N. Characterization and quantification of hydroxycinnamate derivatives in *Stevia rebaudiana* leaves by LC-MS^n. *J. Agric. Food Chem.* **2011**, *59*, 10143–10150. [CrossRef]
7. Peteliuk, V.; Rybchuk, L.; Bayliak, M.; Storey, K.B.; Lushchak, O. Natural sweetener *Stevia rebaudiana*: Functionalities, health benefits and potential risks. *Excli. J.* **2021**, *20*, 1412–1430. [CrossRef]
8. Liu, S.; Xiong, Y.; Cao, S.; Wen, X.; Xiao, H.; Li, Y.; Chi, L.; He, D.; Jiang, Z.; Wang, L. Dietary stevia residue extract supplementation improves antioxidant capacity and intestinal microbial composition of weaned piglets. *Antioxidants* **2022**, *11*, 2016. [CrossRef] [PubMed]
9. Tang, M.; Zhao, J.; Wu, Y.; Yu, C.; Peng, C.; Liu, H.; Cui, Y.; Lan, W.; Lin, Y.; Kong, X.; et al. Improving gut functions and egg nutrition with stevia residue in laying hens. *Poult. Sci.* **2024**, *103*, 103324. [CrossRef]
10. Molina-Barrios, R.M.; Avilés-Trejo, C.R.; Puentes-Mercado, M.E.; Cedillo-Cobián, J.R.; Hernández-Chavez, J.F. Effect of dietary stevia-based sweetener on body weight and humoral immune response of broiler chickens. *Vet. World* **2021**, *14*, 913–917. [CrossRef]
11. Gungor, E.; Altop, A.; Erener, G. Effect of raw and fermented grape seed on growth performance, antioxidant capacity, and cecal microflora in broiler chickens. *Animal* **2021**, *15*, 100194. [CrossRef]

12. Altop, A.; Güngr, E.; Erener, G. *Aspergillus niger* may improve nutritional quality of grape seed and its usability in animal nutrition through solid-state fermentation. *Int. Adv. Res. Eng. J.* **2018**, *2*, 273–277.
13. Jazi, V.; Boldaji, F.; Dastar, B.; Hashemi, S.R.; Ashayerizadeh, A. Effects of fermented cottonseed meal on the growth performance, gastrointestinal microflora population and small intestinal morphology in broiler chickens. *Br. Poult. Sci.* **2017**, *58*, 402–408. [CrossRef]
14. Noura, A.E.F.; Yousseria, M.S.; Ahmed, M.A.; Rehab, M.A.; Dalia, A.M.A. Statistical optimization of chitosan production using marine-derived *Penicillium chrysogenum* MZ723110 in Egypt. *Egypt. J. Aquat. Biol. Fish.* **2021**, *25*, 799–819. [CrossRef]
15. Feng, Z.L.; Du, P.F.; Sheng, Y.Z.; Wang, B.; Chen, W.; Peng, H. Enhanced fumagillin production by optimizing fermentation and purification techniques. *Fermentation* **2024**, *10*, 588. [CrossRef]
16. Bas, D.; Boyaci, I.H. Modeling and optimization I: Usability of response surface methodology. *J. Food Eng.* **2007**, *78*, 836–845. [CrossRef]
17. Myint, K.Z.; Wu, K.; Xia, Y.; Fan, Y.; Shen, J.; Zhang, P.; Gu, J. Polyphenols from *Stevia rebaudiana* (Bertoni) leaves and their functional properties. *J. Food Sci.* **2020**, *85*, 240–248. [CrossRef]
18. *GB/T 6433-2006*; Determination of crude fat in feed. Standards Press of China: Beijing, China, 2006.
19. *GB/T 6434-2006*; Feeding stuffs-Determination of crude fiber content−Method with intermediate filtration. Standards Press of China: Beijing, China, 2006.
20. *GB/T 6438-2007*; Animal feeding stuffs−Determination of crude ash. Standards Press of China: Beijing, China, 2007.
21. Wang, J.R.; Xu, G.F.; Zhao, Y.L.; Su, L.; Hu, K.F.; Li, X. Determination of acid-soluble protein in feed raw materials. In *Proceedings of the 12th Symposium on Animal Nutrition*; China Agricultural University Press: Wuhan, China, 2016; p. 1.
22. Zhai, X.N.; Wang, T.; Liang, L.; Shi, J.F.; Xie, Q.Z.; Sun, H.; Pei, H. Study on optimization and activities of rapeseed meal protein by alkali-extraction and acid-precipitation. *Sci. Technol. Food Ind.* **2022**, *43*, 164–171. [CrossRef]
23. Juanssilfero, A.B.; Kahar, P.; Amza, R.L.; Miyamoto, N.; Otsuka, H.; Matsumoto, H.; Kihira, C.; Thontowi, A.; Yopi; Ogino, C.; et al. Effect of inoculum size on single-cell oil production from glucose and xylose using oleaginous yeast *Lipomyces starkeyi*. *J. Biosci. Bioeng.* **2018**, *125*, 695–702. [CrossRef] [PubMed]
24. Araújo, G.S.; Ribeiro, G.O.; de Souza, S.M.A.; Paulo da Silva, G.; de Carvalho, G.B.M.; Bispo, J.A.C.; Martínez, E.A. Rice (*Oryza sativa*) bran and soybean (*Glycine max*) meal: Unconventional supplements in the mead production. *Food Technol. Biotechnol.* **2022**, *60*, 89–98. [CrossRef] [PubMed]
25. Kumar, M.; Saini, S.; Gayen, K. Exploring the influence of pH on the dynamics of acetone-butanol-ethanol fermentation. *Microorganisms* **2023**, *11*, 1610. [CrossRef] [PubMed]
26. Xu, P.; Tripathi, P.; Mishra, S.; Shu, L.; Li, X.; Zhao, S.; Verma, S.; Verma, R.; Wu, Y.; Yang, Z. Brown sugar as a carbon source can make agricultural organic waste compost enter the secondary thermophilic stage and promote compost decomposition. *Environ. Monit. Assess.* **2024**, *196*, 113. [CrossRef]
27. Zhang, L.; Li, J.; Huo, Y.; Yang, W.; Chen, J.; Gao, Z.; Yang, Z. Ultrasonic extraction and antioxidant evaluation of oat saponins. *Ultrason. Sonochem.* **2024**, *109*, 106989. [CrossRef]
28. Yang, F.; Guo, T.; Zhou, Y.; Han, S.; Sun, S.; Luo, F. Biological functions of active ingredients in quinoa bran: Advance and prospective. *Crit. Rev. Food Sci. Nutr.* **2024**, *64*, 4101–4115. [CrossRef]
29. Chang, Y.; Middleton, R.; Ogawa, Y.; Gregory, T.; Steiner, L.M.; Kovalev, A.; Karanja, R.H.N.; Rudall, P.J.; Glover, B.J.; Gorb, S.N.; et al. Cell wall composition determines handedness reversal in helicoidal cellulose architectures of *Pollia condensata* fruits. *Proc. Natl. Acad. Sci. USA* **2021**, *118*, e2111723118. [CrossRef] [PubMed]
30. Ichikawa, S.; Ichihara, M.; Ito, T.; Isozaki, K.; Kosugi, A.; Karita, S. Glucose production from cellulose through biological simultaneous enzyme production and saccharification using recombinant bacteria expressing the β-glucosidase gene. *J. Biosci. Bioeng.* **2019**, *127*, 340–344. [CrossRef] [PubMed]
31. Isamura, B.K.; Patouossa, I.; Kaba, I.E.; Matondo, A.; Mpiana, P.T. Computational study on the antioxidant activity of five plant food benzoic acid derivatives: Dearomatization and stability of H abstraction radicals. *S. Afr. J. Chem.* **2023**, *77*, 111–118. [CrossRef]
32. Li, X.; Zhang, B.; Hu, Y.; Zhao, Y. New insights into gut-bacteria-derived indole and its derivatives in intestinal and liver diseases. *Front. Pharmacol.* **2021**, *12*, 769501. [CrossRef]
33. Heywood, A.; Lamont, I.L. Cell envelope proteases and peptidases of *Pseudomonas aeruginosa*: Multiple roles, multiple mechanisms. *FEMS Microbiol. Rev.* **2020**, *44*, 857–873. [CrossRef]
34. Sun, W.; Liu, Q.; Chen, H.; Xie, X.; Zhang, Z.; Zeng, Y.; Zhou, J.; Zhou, X.; Jiang, X.; Liang, Z.; et al. Rice phyllospheric *Pantoea* spp. suppress blast and bacterial blight diseases. *Environ. Microbiome* **2025**, *20*, 137. [CrossRef]
35. Žárský, J.; Žárský, V.; Hanáček, M.; Žárský, V. Cryogenian glacial habitats as a plant terrestrialisation cradle—The origin of the anydrophytes and Zygnematophyceae split. *Front. Plant Sci.* **2021**, *12*, 735020. [CrossRef]
36. Ansari, I.; Ejaz, U.; Abideen, Z.; Gulzar, S.; Syed, M.N.; Liu, J.; Li, W.; Fu, P.; Sohail, M. Wild halophytic *Phragmites karka* biomass saccharification by bacterial enzyme cocktail. *Front. Microbiol.* **2021**, *12*, 714940. [CrossRef]

37. Bonfante, P.; Venice, F. Mucoromycota: Going to the roots of plant-interacting fungi. *Fungal Biol. Rev.* **2020**, *34*, 100–113. [CrossRef]
38. Wang, X.J.; Fang, J.N.; Liu, P.; Liu, J.J.; Fang, W.; Fang, Z.M.; Xiao, Y. Mucoromycotina fungi possess the ability to utilize plant sucrose as a carbon source: Evidence from *Gongronella* sp. w5. *Front. Microbiol.* **2021**, *11*, 591697. [CrossRef]
39. Yadav, A.N.; Kour, D.; Kaur, T.; Devi, R.; Yadav, A. Endophytic fungal communities and their biotechnological implications for agro-environmental sustainability. *Folia Microbiol.* **2022**, *67*, 203–232. [CrossRef]
40. Wanmolee, W.; Sornlake, W.; Rattanaphan, N.; Suwannarangsee, S.; Laosiripojana, N.; Champreda, V. Biochemical characterization and synergism of cellulolytic enzyme system from *Chaetomium globosum* on rice straw saccharification. *BMC Biotechnol.* **2016**, *16*, 82. [CrossRef] [PubMed]
41. Tanwar, D.; Sharma, N.; Sharma, N. Evaluation of process parameters for enzymes production from *Trichoderma* sp. Sh2 using pine needles biomass under solid state fermentation. *J. Bio. Innov.* **2020**, *9*, 1501–1519. [CrossRef]
42. Behera, S.S.; El Sheikha, A.F.; Hammami, R.; Kumar, A. Traditionally fermented pickles: How the microbial diversity associated with their nutritional and health benefits? *J. Funct. Foods* **2020**, *70*, 103971. [CrossRef]
43. Ameer, K.; Bae, S.W.; Jo, Y.; Lee, H.G.; Ameer, A.; Kwon, J.H. Optimization of microwave-assisted extraction of total extract, stevioside and rebaudioside-A from *Stevia rebaudiana* (Bertoni) leaves, using response surface methodology (RSM) and artificial neural network (ANN) modelling. *Food Chem.* **2017**, *229*, 198–207. [CrossRef]
44. Lemus-Mondaca, R.; Vega-Gálvez, A.; Zura-Bravo, L.; Ah-Hen, K. *Stevia rebaudiana* Bertoni, source of a high-potency natural sweetener: A comprehensive review on the biochemical, nutritional and functional aspects. *Food Chem.* **2012**, *132*, 1121–1132. [CrossRef]
45. Nath, H.; Samtiya, M.; Dhewa, T. Beneficial attributes and adverse effects of major plant-based foods anti-nutrients on health: A review. *Hum. Nutr. Metab.* **2022**, *28*, 200147. [CrossRef]
46. Réhault-Godbert, S.; Guyot, N.; Nys, Y. The golden egg: Nutritional value, bioactivities, and emerging benefits for human health. *Nutrients* **2019**, *11*, 684. [CrossRef]
47. Hu, W.; He, Z.; Du, L.; Zhang, L.; Li, J.; Ma, Y.; Bi, S. Biomarkers of oxidative stress in broiler chickens attacked by lipopolysaccharide: A systematic review and meta-analysis. *Ecotoxicol. Environ. Saf.* **2023**, *266*, 115606. [CrossRef]
48. Navarro-Hoyos, M.; Bisoyi, R.; Kc, P.; Lutz, N.; Ruxsarash, M. Key Dietary flavonoids: Insights into their structural characteristics, antioxidant and anti-inflammatory activities, and potential as neuroprotective agents. *Molecules* **2026**, *31*, 154. [CrossRef]
49. Hemati, A.; Nazari, M.; Asgari Lajayer, B.; Smith, D.L.; Astatkie, T. Lignocellulosics in plant cell wall and their potential biological degradation. *Folia Microbiol.* **2022**, *67*, 671–681. [CrossRef]
50. Moosmann, B.; Behl, C. Cytoprotective antioxidant function of tyrosine and tryptophan residues in transmembrane proteins. *Eur. J. Biochem.* **2000**, *267*, 5687–5692. [CrossRef]
51. Bouma, G.; van Faassen, M.; Kats-Ugurlu, G.; de Vries, E.G.; Kema, I.P.; Walenkamp, A.M. Niacin (vitamin B_3) supplementation in patients with serotonin-producing neuroendocrine tumor. *Neuroendocrinology* **2016**, *103*, 489–494. [CrossRef]
52. D'Mello, S.A.; Finlay, G.J.; Baguley, B.C.; Askarian-Amiri, M.E. Signaling pathways in melanogenesis. *Int. J. Mol. Sci.* **2016**, *17*, 1144. [CrossRef] [PubMed]
53. Mann, E.R.; Lam, Y.K.; Uhlig, H.H. Short-chain fatty acids: Linking diet, the microbiome and immunity. *Nat. Rev. Immunol.* **2024**, *24*, 577–595. [CrossRef] [PubMed]
54. Xu, X.; Yu, D.; Wang, Y.; Jiang, X.; Lu, F.; Liu, S. Investigating the mechanisms of resveratrol in the treatment of gouty arthritis through the integration of network pharmacology and metabolics. *Front. Endocrinol.* **2024**, *15*, 1438405. [CrossRef] [PubMed]
55. O'Mahony, L.; Akdis, M.; Akdis, C.A. Regulation of the immune response and inflammation by histamine and histamine receptors. *J. Allergy Clin. Immunol.* **2011**, *128*, 1153–1162. [CrossRef] [PubMed]
56. Li, Y.; Liu, N.; Ge, Y.; Yang, Y.; Ren, F.; Wu, Z. Tryptophan and the innate intestinal immunity: Crosstalk between metabolites, host innate immune cells, and microbiota. *Eur. J. Immunol.* **2022**, *52*, 856–868. [CrossRef] [PubMed]
57. Mewa-Ngongang, M.; du Plessis, H.W.; Chidi, B.S.; Hutchinson, U.F.; Ntwampe, K.S.O.; Okudoh, V.I.; Jolly, N.P. Physiological and antagonistic properties of *Pichia kluyveri* for curative and preventive treatments against post-harvest fruit fungi. *Pol. J. Food Nutr. Sci.* **2021**, *71*, 245–253. [CrossRef]
58. Vicente, J.; Calderón, F.; Santos, A.; Marquina, D.; Benito, S. High potential of *Pichia kluyveri* and other *Pichia* species in wine technology. *Int. J. Mol. Sci.* **2021**, *22*, 1196. [CrossRef]

Disclaimer/Publisher's Note: The statements, opinions and data contained in all publications are solely those of the individual author(s) and contributor(s) and not of MDPI and/or the editor(s). MDPI and/or the editor(s) disclaim responsibility for any injury to people or property resulting from any ideas, methods, instructions or products referred to in the content.